Analysis of Three Coupled Defects in One-Dimensional Photonic Bandgap Structure

LIU Dan-Dong(刘丹东)*, CHEN Guang-De(陈光德), XU Zhong-Feng(徐忠锋)

Department of Physics, Xi'an Jiaotong University, Xi'an 710049

(Received 13 October 2005)

The mutual interaction of three different defects in photonic crystals is studied theoretically. A theoretical model based on the classical wave analogue of the tight-binding (TB) picture is applied to the structure. We obtain analytic expressions for the eigenfrequencies and eigenmodes, from which the transmissions at resonance are derived. Based on this, a new type of the photonic quantum-well structure is investigated and its possible application is discussed. The TB predictions are compared with the transfer matrix method simulation results.

PACS: 41. 20. Jb, 42. 55. Tv, 42. 70. Qs

Photonic crystals (PCs) are composite structures with a periodic arrangement of refractive indices. In such materials, there exist photonic band gaps (PBGs), in which the existence of photons is forbidden. By introducing defects into PCs, it is possible to obtain localized modes inside the PBG. Coupled defects have been investigated[1−3] and used in various applications.[4−7]

The tight-binding (TB) method, which was originally developed for electronic systems, has been successfully applied to various photonic structures[8,9] duo to similarity between the Schrödinger equation and Maxwell's equations. In these structures, the eigenmode of each defect is tightly confined to the defect site. The overlap of the modes can provide the propagation of the photons through neighbouring defect sites via hoping.

Using the TB method, analytic expressions for the eigenfrequencies, eigenmodes and dispersion relation corresponding to coupled defects which are identical have been derived.[2,3,10−12] However, theoretical studies of the mutual interaction of different defects and expressions for the transmissions at resonance have seldom been reported. In this Letter, we investigate the PCs with three different defects and obtain the eigenfrequencies and eigenmodes, from which the transmission at resonance is derived.

The model we use in the simulation is a one-dimensional (1D) PC composed of SiO_2 and Si with three SiO_2 defects. The structure is $(HL)^{Ns}\ d_1\ (LH)^N\ L\ d_2\ (LH)^N\ L\ d_3\ (LH)^{Ns}$, where d_1, d_2 and d_3 represent three defects, and the superscripts N_S and N are the period number of the unit. The refractive indices of Si and SiO_2 are $n_H = 3.7$ and $n_L = 1.5$ respectively, and their optical thickness are equal, i.e., $n_H d_H = n_L d_L$. The thickness of the second defect layer is $d_2 = 2.0 d_L$, and the frequency of the corresponding defect mode is $\Omega_2 = 0.2343$. Ω_1 and Ω_3 are chosen to be close to Ω_2 so that its TB parameters α and β are assumed to be equal to those of the PC with identical defects, which can be obtained by substituting the resonant frequencies calculated by the transfer matrix method (TMM) simulation into Eq. (3) in Ref. [11]. The ambient medium is air, and the incident angle is 0°.

We first consider individual localized modes $\boldsymbol{E}_{\Omega 1}(\boldsymbol{r})$, $\boldsymbol{E}_{\Omega 2}(\boldsymbol{r})$ and $\boldsymbol{E}_{\Omega 3}(\boldsymbol{r})$ of three single defects, which satisfy a simplified version of the Maxwell equation

$$\nabla \times [\nabla \times \boldsymbol{E}_{\Omega 1,2,3}(\boldsymbol{r})] = \varepsilon_0(\boldsymbol{r})(\Omega_{1,2,3}/c)^2 \boldsymbol{E}_{\Omega 1,2,3}(\boldsymbol{r}), \tag{1}$$

where $\varepsilon_0(\boldsymbol{r})$ is the dielectric constant of a PC with a single defect, Ω_1, Ω_2 and Ω_3 are the frequencies of the individual localized modes of three single defects. Here it is assumed that $\boldsymbol{E}_{\Omega 1}(\boldsymbol{r})$, $\boldsymbol{E}_{\Omega 2}(\boldsymbol{r})$ and $\boldsymbol{E}_{\Omega 3}(\boldsymbol{r})$ are real, nondegenerate and orthonormal, i.e., $\int d\boldsymbol{r}\varepsilon_0(\boldsymbol{r})\boldsymbol{E}_{\Omega 1}(\boldsymbol{r}) \cdot \boldsymbol{E}_{\Omega 1}(\boldsymbol{r}) = 1$, $\int d\boldsymbol{r}\varepsilon_0(\boldsymbol{r})\boldsymbol{E}_{\Omega 2}(\boldsymbol{r}) \cdot \boldsymbol{E}_{\Omega 2}(\boldsymbol{r}) = 1$, and $\int d\boldsymbol{r}\varepsilon_0(\boldsymbol{r})\boldsymbol{E}_{\Omega 3}(\boldsymbol{r}) \cdot \boldsymbol{E}_{\Omega 3}(\boldsymbol{r}) = 1$.

In the case of three weakly interacting coupled defects, we can express the corresponding eigenmode as a superposition of the individual evanescent defect modes

$$\boldsymbol{E}_\omega(\boldsymbol{r}) = A\boldsymbol{E}_{\Omega 1}(\boldsymbol{r}) + B\boldsymbol{E}_{\Omega 2}(\boldsymbol{r} - \Lambda\hat{\boldsymbol{x}}) + C\boldsymbol{E}_{\Omega 3}(\boldsymbol{r} - 2\Lambda\hat{\boldsymbol{x}}), \tag{2}$$

where Λ is the distance between neighbouring defects. The eigenmode $\boldsymbol{E}_\omega(\boldsymbol{r})$ also satisfies Eq. (1) where $\varepsilon_0(\boldsymbol{r})$ is replaced with the dielectric constant of the coupled system $\varepsilon(\boldsymbol{r}) \approx \varepsilon(\boldsymbol{r} - \Lambda\hat{\boldsymbol{x}}) \approx \varepsilon(\boldsymbol{r} - 2\Lambda\hat{\boldsymbol{x}})$, and $\Omega_{1,2,3}$ replaced with eigenfrequency ω of the coupled defects,

$$\nabla \times [\nabla \times \boldsymbol{E}_\omega(\boldsymbol{r})] = \varepsilon(\boldsymbol{r})(\omega/c)^2 \boldsymbol{E}_\omega(\boldsymbol{r}). \tag{3}$$

Multiplying both the sides of Eq. (3) first by $\boldsymbol{E}_{\Omega 1}(\boldsymbol{r})$, then by $\boldsymbol{E}_{\Omega 2}(\boldsymbol{r} - \Lambda\hat{\boldsymbol{x}})$ and by $\boldsymbol{E}_{\Omega 3}(\boldsymbol{r} - 2\Lambda\hat{\boldsymbol{x}})$ respectively and spatially integrating the resulting

* Email: dandangliu@mail.xjtu.edu.cn

©2005 Chinese Physical Society and IOP Publishing Ltd

equations respectively, we obtain the analytic expressions for the eigenfrequencies and eigenmodes for $\Omega_1 = \Omega_3 \neq \Omega_2$ and $\Omega_1 \approx \Omega_2 \neq \Omega_3$. For simplicity, the field patterns of three localized modes $\boldsymbol{E}_{\Omega 1}(\boldsymbol{r})$, $\boldsymbol{E}_{\Omega 2}(\boldsymbol{r})$ and $\boldsymbol{E}_{\Omega 3}(\boldsymbol{r})$ are assumed to be the same when Ω_1, Ω_2 and Ω_3 are close enough.

Firstly, the eigenfrequencies corresponding to coupled defects for $\Omega_1 = \Omega_3 \neq \Omega_2$ are given by

$$\omega_1 = \Omega_3, \tag{4}$$

$$\omega_2 = \Omega_2\sqrt{1 - \frac{2\beta(\beta-\alpha)\Omega_3^2}{\Omega_3^2 - \Omega_2^2}}, \tag{5}$$

$$\omega_3 \approx \Omega_3\sqrt{1 + \frac{2\beta(\beta-\alpha)\Omega_2^2}{\Omega_3^2 - \Omega_2^2}}, \tag{6}$$

where $\alpha = \int d\boldsymbol{r}\varepsilon(\boldsymbol{r})\boldsymbol{E}_{\Omega 1}(\boldsymbol{r}) \cdot \boldsymbol{E}_{\Omega 2}(\boldsymbol{r} - \Lambda\hat{\boldsymbol{x}})$ and $\beta = \int d\boldsymbol{r}\varepsilon_0(\boldsymbol{r} - \Lambda\hat{\boldsymbol{x}})\boldsymbol{E}_{\Omega 1}(\boldsymbol{r}) \cdot \boldsymbol{E}_{\Omega 2}(\boldsymbol{r} - \Lambda\hat{\boldsymbol{x}})$. Corresponding to eigenfrequencies ω_1, ω_2 and ω_3, the coefficients in Eq. (2) are given respectively by

$$C = -A, \quad B = 0, \tag{7}$$

$$C = A, \quad B \approx \frac{\Omega_3^2 - \Omega_2^2}{(\alpha-\beta)\Omega_2^2}A, \tag{8}$$

$$C = A, \quad B \approx 0. \tag{9}$$

Table 1 gives a comparison between the resonant frequencies calculated by the TMM simulation and values obtained by using Eqs. (4)–(6) for $\Omega_1 = \Omega_3 = 0.2484$ and $N_{\mathrm{S}} = 2$. Equations (4), (5) and (6) indicate that ω_1 changes slightly, and ω_2 and ω_3 are closer to Ω_2 and Ω_3 respectively with increasing the defect separation, i.e., decreasing α and β, which can cause a degeneration of ω_3 and ω_1 due to $\omega_1 = \Omega_3$. The TB predictions coincide well with the TMM simulation results.

Table 1. Comparison between the eigenfrequencies obtained by using Eqs. (4)–(6) and the TMM simulation results for $\Omega_1 = \Omega_3 = 0.2484$ and $N_{\mathrm{S}} = 2$.

	$N=2$		$N=3$		$N=4$	
	TMM	TB	TMM	TB	TMM	TB
ω_2	0.2318	0.2311	0.2338	0.2338	0.2342	0.2342
ω_3	0.2511	0.2513	0.2485^a	0.2488	0.2483^a	0.2484
ω_1	0.2483	0.2484		0.2484		0.2484

[a] ω_1 and ω_3 degenerate.

We obtain $|A| = |C|$ from Eqs. (7)–(9), which indicates that the transmissions at resonant frequencies ω_1, ω_2 and ω_3 equal to 1. This can be explained as follows. The magnitude of the incident electric field is assumed to be 1. The electric field magnitudes a_{d3} and b_{d3} of plane waves propagating toward right and left at the third defect are related to the magnitude of the output electric field by a matrix

$$\begin{pmatrix} a_{d3} \\ b_{d3} \end{pmatrix} = M \begin{pmatrix} \sqrt{T_\omega}e^{i\varphi_t} \\ 0 \end{pmatrix} = \begin{pmatrix} f & g \\ h & j \end{pmatrix} \begin{pmatrix} \sqrt{T_\omega}e^{i\varphi_t} \\ 0 \end{pmatrix},$$
$$A_{d3} = |a_{d3}| + |b_{d3}| = (|f| + |h|)\sqrt{T_\omega}, \tag{10}$$

where M is the transfer matrix of the right of the third defect, A_{d3} is the maximum magnitude at the third defect. Similarly, we have

$$\begin{pmatrix} a_{d1} \\ b_{d1} \end{pmatrix} = \begin{pmatrix} f & g \\ h & j \end{pmatrix} \begin{pmatrix} 1 \\ \sqrt{1-T_\omega}e^{i\varphi_r} \end{pmatrix},$$
$$A_{d1} = |a_{d1}| + |b_{d1}| = |f + g\sqrt{1-T_\omega}e^{i\varphi_r}| + |h + j\sqrt{1-T_\omega}e^{i\varphi_r}|, \tag{11}$$

where a_{d1} and b_{d1} are the magnitudes of plane waves propagating toward right and left at the first defect, and A_{d1} is the maximum magnitude at the first defect. We derive $A_{d1} = A_{d3}$ from $|A| = |C|$ and then $T_\omega = 1$ from Eqs. (10) and (11). Figure 1 shows the transmission spectra calculated by the TMM simulation at $N = 2, 3, 4$ for $N_{\mathrm{S}} = 2$ and $\Omega_1 = \Omega_3 = 0.2484$. All the transmissions at resonance equal to 1 for $N = 2$, but the transmission at the resonant frequencies except for ω_2 is less than 1 for $N = 3$ and 4. This is explained as follows. With the defect separation increasing, the overlap of the localized modes decreases so that the overlap is not enough to provide the complete propagation of the photons through the first and third defect sites and to enable the defect mode to split. Therefore, the corresponding transmission at resonance becomes smaller with the increasing defect separation, which is analogous to that of PCs with two identical defects.

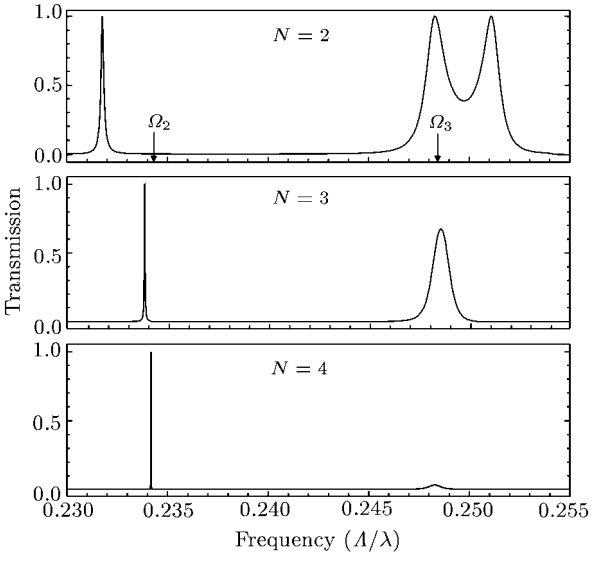


Fig. 1. Transmission spectra calculated by the TMM simulation at $N = 2, 3, 4$ for $N_{\mathrm{S}} = 2$ and $\Omega_1 = \Omega_3 = 0.2484$.

Secondly, we consider the eigenfrequencies and transmission at resonance when Ω_1 is very close to Ω_2 but is not equal to Ω_3. We obtain the eigenfrequencies as

$$\omega' = \sqrt{\frac{(\Omega_1^2 + \Omega_2^2) + \sqrt{(\Omega_1^2 - \Omega_2^2)^2 + 4\beta^2\Omega_1^2\Omega_2^2}}{2(1-\alpha^2)}}, \tag{12}$$

$$\omega'' = \sqrt{\frac{(\Omega_1^2+\Omega_2^2) - \sqrt{(\Omega_1^2-\Omega_2^2)^2 + 4\beta^2\Omega_1^2\Omega_2^2}}{2(1-\alpha^2)}}, \tag{13}$$

$$\omega_3 = \Omega_3\sqrt{1+\frac{\beta^2\Omega_2^2}{\Omega_3^2-\Omega_2^2}}. \tag{14}$$

When $\Omega_1 > \Omega_2$, ω_2 is less than Ω_2 due to the coupling of localized modes of the first and second defect and then its expression is Eq. (13). Otherwise, the expression of ω_2 is Eq. (12).

Corresponding to ω' and ω'', C/A are given respectively by

$$\frac{C}{A} = \frac{(\Omega_1^2-\Omega_2^2) - \sqrt{(\Omega_1^2-\Omega_2^2)^2+4\beta^2\Omega_1^2\Omega_2^2}}{(2\Omega_3^2-\Omega_1^2-\Omega_2^2) - \sqrt{(\Omega_1^2-\Omega_2^2)^2+4\beta^2\Omega_1^2\Omega_2^2}}, \tag{15}$$

$$\frac{C}{A} = \frac{(\Omega_1^2-\Omega_2^2) + \sqrt{(\Omega_1^2-\Omega_2^2)^2+4\beta^2\Omega_1^2\Omega_2^2}}{(2\Omega_3^2-\Omega_1^2-\Omega_2^2) + \sqrt{(\Omega_1^2-\Omega_2^2)^2+4\beta^2\Omega_1^2\Omega_2^2}}. \tag{16}$$

Table 2 shows the resonant frequencies calculated by the TMM simulation and values obtained by using Eqs. (12)–(14) for $\Omega_1 = \Omega_2 = 0.2343$, $\Omega_3 = 0.2484$ and $N_S = 2$. With the increasing defect separation, eigenfrequencies ω' and ω'' are closer to Ω_2, and ω_3 is closer to Ω_3.

Table 2. Comparison between the eigenfrequencies obtained by using Eqs. (12)–(14) and the TMM simulation results for $\Omega_1 = \Omega_2 = 0.2343$, $\Omega_3 = 0.2484$ and $N_S = 2$.

	$N=2$		$N=3$		$N=4$	
	TMM	TB	TMM	TB	TMM	TB
ω_1	0.2291	0.2308	0.2323	0.2329	0.2335	0.2338
ω_2	0.2379	0.2377	0.2359	0.2356	0.2349	0.2347
ω_3	0.2499	0.2500	0.2485	0.2486	0.2483	0.2484

Now, we consider the transmission at resonance. The magnitude of the incident electric field is assumed to be 1. The ratio of the output electric field magnitude to the maximum magnitude of the field intensity at the third defect is denoted by η, which can be derived from Eq. (10). The magnitude of the output electric field is written as

$$\boldsymbol{A}_{\rm out} = A_{d_1}\left|\frac{C(\boldsymbol{E}_{\Omega 3}(\boldsymbol{r}-2\Lambda\hat{\boldsymbol{x}}))_{\rm MAX}}{A(\boldsymbol{E}_{\Omega 1}(\boldsymbol{r}))_{\rm MAX}}\right|\eta,$$

where $(\boldsymbol{E}_{\Omega 1}(\boldsymbol{r}))_{\rm MAX}/(\boldsymbol{E}_{\Omega 3}(\boldsymbol{r}-2\Lambda\hat{\boldsymbol{x}}))_{\rm MAX}$ is assumed to be equal to 1 because Ω_1 and Ω_3 are close. The TMM simulation results show $(\boldsymbol{E}_{\Omega 1}(\boldsymbol{r}))_{\rm MAX}/(\boldsymbol{E}_{\Omega 3}(\boldsymbol{r}-2\Lambda\hat{\boldsymbol{x}}))_{\rm MAX} = 1.03$ at $\Omega_1 = 0.2343$ and $\Omega_3 = 0.2484$. The transmission T_ω at the resonant frequency ω equal to $|A_{\rm out}|^2$, which is given by

$$T_\omega = \left(\frac{C}{A}\right)^2(\eta A_{d1})^2 = \left(\frac{C}{A}\right)^2 c, \tag{17}$$

where c is a constant, which is determined by inserting the transmission T_ω obtained by the TMM simulation into Eq. (17).

Figure 2 gives the transmission at ω_2 as a function of Ω_1 for $N_S = 2$, $N = 4$ and $\Omega_3 = 0.2484$ and for $N_S = 3$, $N = 6$ and $\Omega_3 = 0.2411$. The lines are calculated by substituting Eqs. (15) and (16) into Eq. (17), and the circles are obtained by using the TMM simulation. The TB predictions are in excellent agreement with the TMM simulation results when Ω_1 is very close to Ω_2. From Fig. 2, it is obvious that the transmission has its minimum value at $\Omega_1 = \Omega_2$ when β is small, which is derived from Eqs. (17) and (15) or (16) to be

$$T_{\omega\,\rm MIN} = \left(\frac{\beta\Omega_2^2}{\Omega_3^2-\Omega_2^2}\right)^2 c, \tag{18}$$

which is dependent of β and $\Omega_3^2 - \Omega_2^2$.

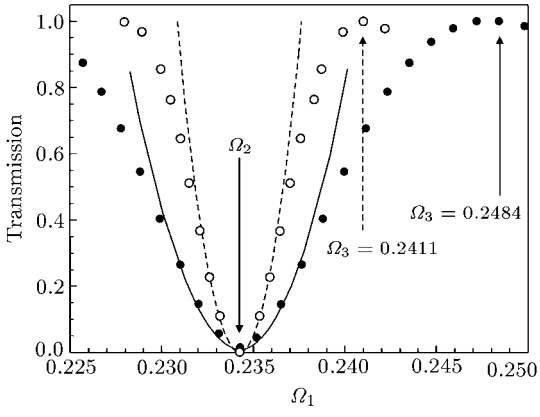


Fig. 2. Transmission at resonant frequency ω_2 as a function of Ω_1 for $N_S = 2$, $N = 4$ and $\Omega_3 = 0.2484$ (solid lines and solid circles) and for $N_S = 3$, $N = 6$ and $\Omega_3 = 0.2411$ (dashed lines and open circles). The circles represent the TMM simulation results. The lines are obtained by using Eqs. (15)–(17).

Ω_1 ranging between Ω_3 and Ω_2, the transmission T_ω varies from 1 to its minimum value $T_{\omega\,\rm MIN}$. Therefore, decreasing the difference between Ω_2 and Ω_3 can improve the sensitivity of the transmission T_ω to Ω_1. It can cause an increase of the minimum transmission $T_{\omega\,\rm MIN}$. To avoid increasing $T_{\omega\,\rm MIN}$, we decrease β by increasing the defect separation. Figure 2 shows that the transmission at resonance is more sensitive to Ω_1 for $\Omega_3 = 0.2411$ than $\Omega_3 = 0.2484$, and the minimum transmission $T_{\rm MIN}$ for $N_S = 3$ and $N = 6$ is smaller than that for $N_S = 2$ and $N = 4$.

Figure 3 shows the natural logarithm of the transmission at ω_1 as a function of Ω_1 for $N_S = 2$, $N = 4$ and $\Omega_3 = 0.2484$ and for $N_S = 3$, $N = 6$ and $\Omega_3 = 0.2411$. The transmission at ω_1 has its maximum values at $\Omega_1 = \Omega_2$ and $\Omega_1 = \Omega_3$. The TB predictions are in excellent agreement with the TMM simulation results. This good agreement shows that the TB formalism and the assumption that the field patterns of three localized modes are the same are valid for our structure.

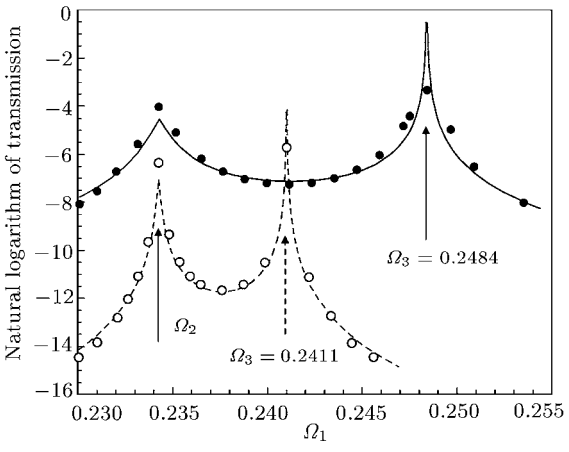


Fig. 3. Natural logarithm of transmission at resonant frequency ω_1 as a function of Ω_1 for $N_S = 2$, $N = 4$ and $\Omega_3 = 0.2484$ (solid lines and solid circles) and for $N_S = 3$, $N = 6$ and $\Omega_3 = 0.2411$ (dashed lines and open circles). The circles represent the TMM simulation results. The lines are obtained by using Eqs. (15)–(17).

When Ω_1 is between Ω_2 and Ω_3, the transmission at the eigenfrequency ω_1, which is not less than the transmission at ω_3, is far less than that at ω_2 except for $\Omega_1 = \Omega_2$.

When $\Omega_1 = \Omega_3 \neq \Omega_2$, there is only a complete transmission peak around Ω_2 in the PBG for $N = 3$ and 4. This is explained as follows. The structure is composed of three PCs each with a defect whose PBG are identical but defect modes are different. For the electromagnetic (EM) wave with the frequency of the defect mode of the middle PC, two surrounding PCs strongly prohibit its propagation and play roles of barriers, whereas the middle PC sustains its propagation and acts as a well. The photonic quantum-well (QW) structure is formed and the EM wave is highly confined to the middle PC, especially to the defect in the middle PC (see Eq. (8)). Therefore, the overlap of the localized modes is enough to provide the propagation of the photons through neighbouring defect sites via hopping. A complete transmission is observed around the frequency of the defect mode of the middle PC, i.e., Ω_2.

Tuning Ω_1 to Ω_2, only a surrounding PC prohibits the propagation of the EM wave with frequency of the defect mode in the middle PC. The photonic QW structure completely vanishes. Consequently the transmission at resonance around Ω_2 approaches its minimum value.

This provides a mechanism for optical switches, whose efficiency and sensitivity can be improved by decreasing $\Omega_3 - \Omega_2$ and increasing the defect separation. For the input light with frequencies even extending throughout the PBG, the intensity of the output light with a narrow band of frequencies can be tuned by using the structure. It is different from optical switches realized by a periodic modulation of defects in a PC,[4] a shift of band edge,[13] and a shift of defect modes,[14] which require that the input light must be limited in a narrow range of frequency. As compared with the optical switch using two defects in series,[15] the transmission at resonance of this structure can reach 1 due to high confinement of EM wave.

In conclusion, the transmission properties of the PCs with three different defects have been investigated by using the TB method, which is a useful tool to investigate the mutual interaction of defects in structures. This study is crucial to the design and characterization of these PCs.

References

[1] Bayindir M, Temelkuran B et al 2000 *Phys. Rev. Lett.* **84** 2140
[2] Leuenberger D, Ferrini R et al 2004 *J. Appl. Phys.* **95** 806
[3] Lan S, Nishikawa S et al 2002 *Phys. Rev.* B **65** 165208
[4] Lan S and Nishikawa S 2001 *Appl. Phys. Lett.* **78** 2101
[5] Bayindir M and Ozbay E 2001 *Phys. Rev.* B **63** 08110708-1
[6] Zhu S Y, Liu N H et al 2000 *Opt. Commun.* **174** 139
[7] Li Y H, Jiang Ha T et al 2004 *Chin. Phys. Lett.* **21** 1976
[8] de Srerke C M 1998 *Phys. Rev.* E **57** 3502
[9] Lidofikis E, Sigalas M M et al 1998 *Phys. Rev. Lett.* **81** 1405
[10] Bayindir M, Temelkuran B et al 2000 *Phys Rev.* B **61** R11855
[11] Bayindir M, Kural C et al 2001 *J. Opt. A: Pure Appl. Opt.* **3** S184
[12] Huang X Q and Cui Y P 2003 *Chin. Phys. Lett.* **20** 1721
[13] Scalora M and Dowing J P 1994 *Phys. Rev. Lett.* **73** 1368
[14] Jiang H T and Chen H 2004 *Chin. Phys. Lett.* **21** 101
[15] Villeneuve P R and Abrams D S 1996 *Opt. Lett.* **15** 2017